atmosphere

MDPI

Article

Modelling the Atmospheric Environment Associated with a Wind-Driven Fire Event in Portugal

Carolina Purificação [1,2,3,*], Nuno Andrade [1,3,4], Miguel Potes [1,2,3], Vanda Salgueiro [1,2,3], Flavio T. Couto [1,2,3] and Rui Salgado [1,2,3,5]

[1] Instituto de Ciências da Terra (ICT), Rua Romão Ramalho 59, 7000-671 Évora, Portugal; nuno.andrade@uevora.pt (N.A.); mpotes@uevora.pt (M.P.); vsalgueiro@uevora.pt (V.S.); fcouto@uevora.pt (F.T.C.); rsal@uevora.pt (R.S.)
[2] Instituto de Investigação e Formação Avançada (IIFA), Universidade de Évora, Palácio do Vimioso, Largo Marquês de Marialva, Apart. 94, 7002-554 Évora, Portugal
[3] Earth Remote Sensing Laboratory (EaRS Lab.), Rua Romão Ramalho 59, 7000-671 Évora, Portugal
[4] Escola de Ciências Sociais, Colégio do Espírito Santo, Universidade de Évora, Largo dos Colegiais 2, 7000-645 Évora, Portugal
[5] Departamento de Física, Escola de Ciência e Tecnologia, Universidade de Évora, Rua Romão Ramalho 59, 7000-671 Évora, Portugal
* Correspondence: ana.purificacao@uevora.pt

Abstract: Increased knowledge of the meteorological conditions that lead to mega-fires is important to prevent wildfires and improve firefighting. This study analyses the atmospheric conditions that led to the largest forest fire ever observed in Portugal in 2019. The fire burned an estimated total area of around 9000 hectares in 12 h. The study is based on two simulations performed with the Meso-NH atmospheric model. The control simulation was configured in a single and large domain with 2500 m resolution, whereas a second simulation was configured using the grid nesting technique with an inner domain with 500 m resolution. The fire developed under typical summer conditions, under the influence of the Azores anticyclone and the presence of the Iberian thermal low. The weather pattern included intense northwest winds in the western region of the Iberian Peninsula. In the fire area, the wind speed was around 7 m s^{-1} with maximum wind gusts of 15 m s^{-1}, favouring the rapid spread of the fire and characterising the event as a wind-driven fire. This study demonstrates the benefits of the use of large domains and high-resolution numerical simulations to explore the regional and local effects, which are crucial for the evolution of some fires.

Keywords: wind-driven fires; orographic effects; fire weather conditions; Meso-NH model

check for updates

Citation: Purificação, C.; Andrade, N.; Potes, M.; Salgueiro, V.; Couto, F.T.; Salgado, R. Modelling the Atmospheric Environment Associated with a Wind-Driven Fire Event in Portugal. *Atmosphere* **2022**, *13*, 1124. https://doi.org/10.3390/atmos13071124

Academic Editors: Stergios Kartsios, Ioannis Pytharoulis and Theodore Karacostas

Received: 17 May 2022
Accepted: 11 July 2022
Published: 15 July 2022

1. Introduction

Atmospheric conditions are a dominant factor in fire spread and intensity at several spatial and temporal scales [1,2], sometimes leading to extreme forest fires with large and destructive effects [3]. Additionally, complex terrain can significantly influence meteorological conditions due to the interactions with the atmospheric flow. Such interactions are crucial in extreme fire behaviour [4,5]. For example, many extreme fires are due to the interaction of the fire front with the environmental conditions found in a mountainous landscape, which can increase the rate of propagation of the fire front [6,7].

The important role played by orography in fire evolution has been extensively documented over the last century. However, the importance of the orography in creating fire weather conditions is still considered an open field in the context of mountain meteorological phenomena [8,9]. Nowadays, the fundamentals of the mountain meteorological phenomena that affect fire behaviour are better understood and known as diurnal mountain winds, dynamic channelling, Foehn winds, low-level jets, and mountain waves [10].

In general, strong winds can favour wind-driven fires, which are characterised by the head of the fire being spread faster by the wind in the centre than on the flanks of the fire [11]. Many wind-driven fires occur in coastal mountainous regions, for example, California [12,13], France [14], and Greece [15,16], all of which present a complex terrain and a Mediterranean climate with hot and dry summers.

Considering the synoptic conditions associated with the occurrence of large fires in France during recent decades (1973–2013), [14] showed that most of the large fires occurred under the 'Atlantic Ridge' synoptic weather type, which combines an anticyclone ridge over the eastern Atlantic and a cyclonic anomaly stretching from the North Sea to Central/Eastern Europe and the Mediterranean basin. In Portugal, the frequent development of the Iberian low thermal system in the summer [17,18] increases the pressure gradients between the Iberia centre and the anticyclone ridge over the Atlantic, inducing strong winds which create favourable conditions for fire spread.

Nauslar et al. (2018) [19] carried out a study to characterise the meteorological factors that drove two extreme wind-driven fire events in California in 2017. The authors highlighted the important roles that both climate variability and meteorological factors have on extreme fires in terms of preconditioning fuel abundance, flammability, and driving fire spread. Recently, a study about significant forest fires on Madeira Island [20], using high-resolution numerical simulations, stressed the impact of the orography, mainly through the generation of a deep Foehn effect. The study showed the importance of this effect on the development of large forest fires in the lowest regions of the island.

In recent years, some studies have aimed to study fire–atmosphere interactions over complex terrain using several techniques, including the coupling of fire and atmospheric models [21–24]. A coupled simulation may reproduce the total burnt area, showing the predominance of wind-driven propagation, in which the fire behaviour is mainly driven by the mean flow [16].

Portugal has the highest total number of fires and the second-largest total burned area in Europe [25]. The fire seasons of 2003 and 2005 [26,27], as well as the mega-fires of June [28,29] and October 2017 [30], showed the vulnerability of the country to the occurrence of such extreme events. The episodes had a high impact on social (dozens of fatalities), economic, and environmental levels. In general, these extreme fire events are associated with extreme meteorological conditions [28,31] or climatic phenomena, such as intense heat waves, as verified by the fire season of 2003 [26,32].

Some mega-fires occur without extreme meteorological conditions and should be studied to understand how the fire propagates in a short time period. For example, the largest forest fire in Portugal, which occurred in 2019, was characterised by a rapid spread and burned approximately 20 km in length in the first 12 h [33]. The smoke plume was unusually extensive and was detected in southern Portugal [34]. This episode in Vila de Rei county has been considered in order to understand the atmospheric environment associated with a forest fire occurring over complex terrain from simulations with convection explicitly resolved.

The high-resolution simulations resolve fine-scale meteorological processes, including convection, clouds' microphysics, and surface forcing, which is poorly represented in coarse-resolution global models. The use of high resolution improves the complex topography representation, land–sea contrast, and land cover heterogeneities. The atmospheric model used in the present study, the Meso-NH, can be used to perform simulations in LES mode, which should be studied as a fine representation of the atmospheric effects of surface fluxes, namely those produced by fires and the consequent retroactive effects, as shown in [35], a numerical study about the Aullene wildfire that occurred on the mountainous island of Corsica.

Moreover, this study aims to complement previous studies developed under the "Iberian Centre for Research and Forest Firefighting" framework (CILIFO, www.cilifo.eu, last accessed 29 June 2022), namely in the context of characterisation of meteorological environments of historical wildfires [20,28].

The paper is organised as follows. Section 2 presents the study region, as well as the data used and modelling aspects. In Section 3, the results are presented, followed by the discussion in Section 4. The conclusions are given in Section 5.

2. Study Area and Data Sources

2.1. Study Area

Vila de Rei is located in the centre of Portugal at 39°40′31.08″ N; 8°8′48.444″ W (Figure 1c). The regional geography contributes to the local climate, which is Mediterranean with continental influences. July is the windiest month, with an average hourly wind speed of 3.5 m/s, and the wind direction is predominantly from the north [36].

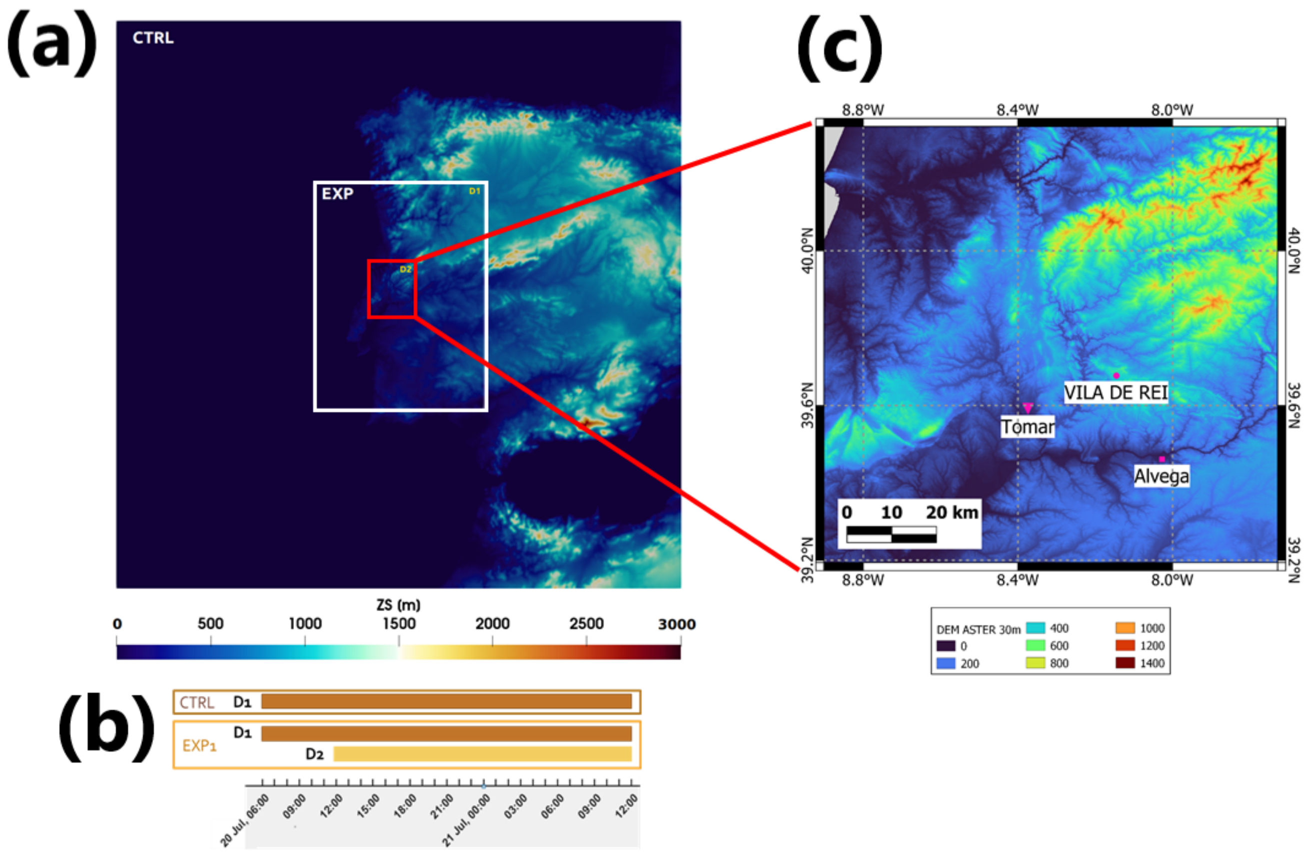

Figure 1. (**a**) Meso-NH configuration and Vila de Rei location with orography obtained from the SRTM database with the large domain at 2500 m resolution (CTRL and EXPD1) and the inner domain at 500 m (EXPD2) resolution; (**b**) Timeline of the period simulated in the larger and inner domains; (**c**) Study Region—Map of local orography from Advanced Spaceborne Thermal Emission and Reflection Radiometer (ASTER), Global Digital Elevation Model (GDEM)—Version 3.

The local terrain was analysed with data from the Advanced Spaceborne Thermal Emission and Reflection Radiometer (ASTER), Global Digital Elevation Model (GDEM)—Version 3, with a spatial resolution of 1 arc second, approximately 30-m horizontal posting at the equator. The region of Vila de Rei is surrounded by hills and valleys with large differences in altitude (500 m). Further from the village, a ridge of bigger mountains is located to the north and northeast, and a smaller mountain is located to the west and southwest (Figure 1c).

The years 1986 and 2017 were marked by large wildfires in the Vila de Rei region, when more than 12,000 ha and 19,000 ha burned, respectively [37–39]. The present case study is the wildfire that occurred on 20 July 2019. It started at 1500 UTC with a total burnt area of 9249 ha.

2.2. Data Sources

To understand the environment associated with large fires, it is recommended to use results from limited-area meteorological models. For example, a set of procedures adopted for forest fires based on the safety protocol, "Lookouts, Anchor Points, Communications, Escape Route, and Safety Zones (LACES)", are used by the National Authority of Civil Protection to implement safety procedures and to prevent serious accidents in wildfire suppression [40]. The contribution of scientific research performs a major role in this regard. It can fit from the anchor points and escape routes based on the knowledge of fire weather conditions and orographic effects to define strategies before and during firefighting, as provided to changes in these factors [41]. To analyse the meteorological conditions during the event, different data were used. In this subsection, the observation of data used is presented, as well as the numerical experiments that complement the observations.

2.2.1. Meteorological Data

Data from the national automatic weather stations network were obtained from the Portuguese Institute for Sea and Atmosphere (IPMA) for 20 and 21 July 2019. Two meteorological stations near the fire area, namely Alvega (39°27′39.97″ N; 8°1′37.09″ W) and Tomar (39°35′31.66″ N; 8°22′26.31″ W), were used in the study, as indicated in Figure 1c. The data from the atmospheric sounding launched in Lisbon (38°45′58.260″ N; 9°7′42.430″ W) at 1200 UTC on 20 July 2019 was obtained from the University of Wyoming (https://weather.uwyo.edu/upperair/sounding.html, accessed on 30 May 2022).

Images of the High-Resolution Visible (HRV) channel, with a sampling distance at a nadir of 1 km and time resolution of 15 min, of the Spinning Enhanced Visible and InfraRed Imager (SEVIRI) onboard geostationary Meteosat satellites are also used in the study. The data were obtained from the Earth Observation Portal (https://eoportal.eumetsat.int/, accessed on 17 May 2022).

The mean sea level pressure and surface wind speed fields were downloaded from the European Centre for Medium-Range Weather Forecasts (ECMWF) reanalysis, namely the ERA5 dataset (https://cds.climate.copernicus.eu/, accessed on 17 December 2021).

2.2.2. Numerical Modelling

The study is based on atmospheric modelling with the Meso-NH model. It is a mesoscale non-hydrostatic research model developed by the Centre National de Recherches Météorologiques (CNRM/Météo-France) and the Laboratoire d'Aérologie (http://mesonh.aero.obs-mip.fr/mesonh55/, accessed on 13 September 2021). The model can run real cases or idealised cases in 3D, 2D, or 1D form. It is a set of prognostic variables, includes the potential temperature θ, the pressure, the subgrid turbulent kinetic energy, three velocity components, and the mixing ratios of up to seven hydrometeors species (vapour, cloud droplets, raindrops, ice crystals, snow, graupel, and hail). The model runs under the anelastic approximation and solves the conservation equations of mass, momentum, humidity, scalar variables, and the thermodynamic equation [42].

The model was run over a large domain, with 500 × 500 grid points and a horizontal resolution of 2500 m, with the main objective of characterising the peninsular scale flow, namely the development of the west Iberian sea breeze system and thermal low. This simulation is called the control simulation (CTRL); see Figure 1a. In order to study the local circulation, a second simulation (EXP) was performed over a smaller domain, using the grid-nesting technique. As shown in Figure 1a, the coarser domain has a horizontal resolution of 2500 m (D1: 150 × 200 grid points), and the inner domain has a 500 m resolution (D2: 200 × 250 grid points). For the inner domain, the higher resolution is used to better represent the complex terrain characteristics of the region. The model orography is built from the Shuttle Radar Topography Mission (SRTM) database. The surface is characterised using the ECOCLIMAP vegetation database and the FAO soil texture database (sand and clay) [43]. The vertical configuration was established with

50 stretched levels by the model and following the topography. The simulations were initialised and forced using the ECMWF operational analysis, updated every 6 h.

The physical configuration of the model is similar to those successfully used in previous studies [20] using the schemes shown in Table 1. For the turbulence, in the inner 500 m resolution domain, the full 3D turbulent fluxes scheme was activated, while in the 2500 m domain, only the vertical fluxes were considered (1D scheme) [44,45]. The deep convection was not parametrised, while the shallow convection was parameterised only in the larger domain using the EDKF scheme [46]. The clouds microphysics was parametrised in both domains with a scheme that considers five types of hydrometeors (ICE3) [47]. Finally, the surface fluxes were computed using the externalised SURFEX model coupled to the Meso-NH [48].

Table 1. Parametrisations schemes used in the present study by the Meso-NH model.

	CTRL	EXP	
Parametrization	**2500 m**	**2500 m**	**500 m**
Turbulence	1D	1D	3D
Convection	None	None	None
Shallow convection	EDKF	EDKF	None
Cloud microphysics	ICE3	ICE3	ICE3
Radiation	ECMWF	ECMWF	ECMWF

The CTRL was run between 0600 UTC on 20 July and 1200 UTC on 21 July. For the EXP, the model was initiated at 0600 UTC on 20 July only for the larger domain, whereas the inner domain run started at 1200 UTC on 20 July (Figure 1b), both ending at 1200 UTC on 21 July 2019.

3. Results

3.1. Overview of the Fire Event

The land cover information for the burned area is available in Figure 2a. The data used is from the Corine Land Cover (CLC), the 5th CLC inventory (CLC2018), coordinated by the European Environment Agency (EEA), which presents 44 land cover classes with a minimum mapping unit of 24 hectares. The major classes found in the burned area were 324 (transitional woodland/shrub) and 322 (moors and heathland), which together represent 83% of the burned area (Figure 2a). The land cover classes were converted into types of fuel models according to the Northern Forest Fire Laboratory (NFFL) classification, presented in [49]. In Table 2, the correspondences between CLC classes and fuel types are described (adapted from [16]).

Table 2. Conversion matrix of CLC 2012 land uses to NFFL fuel models (Adapted from [16]).

CLC Code	NFFL Fuel Model	Description
121	14	No fuel
241	3	Tall grass (76 cm)
242	1	Short grasses (30 cm)
243	7	Southern rough
311	9	Hardwood litter
312	10	Timber (litter and understory)
322	6	Dormant brush, hardwood slash
324	7	Southern rough

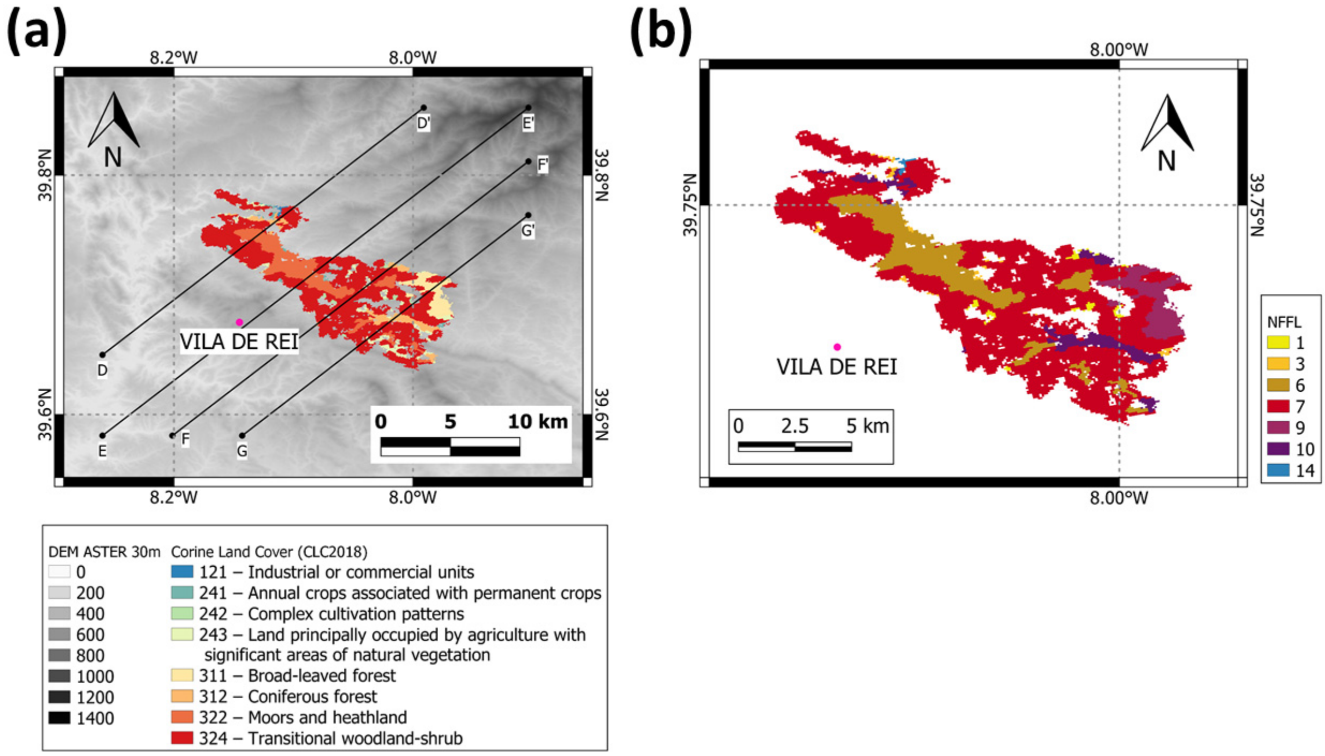

Figure 2. (**a**) Corine Land Cover from the 5th CLC inventory (CLC2018) for the total burnt area. The SW–NE vertical cross-sections are marked as D–D′, E–E′, F–F′ and G–G′. These cross-sections are used for the wind speed analysis given in Section 3.4; (**b**) Fuel models presented in the burned area according to the Northern Forest Fire Laboratory (NFFL) classification presented in [49].

Figure 2b shows the fuel models present in the burned area. The majority of the burned area is represented by 2 fuel models: 6—dormant brush, hardwood slash and 7—southern rough. Both are from the group brush, according to [49]. They represent 87% of the fuel in the Vila de Rei wildfire and correspond to 70% pine trees and 17% eucalyptus [34].

According to the satellite image (Figure 3a), a smoke plume with two distinct directions was observed in the late afternoon of 20 July 2019, going south-eastward and north-eastward and creating a "butterfly shape". Figure 3b displays the Skew-T/Log-P diagram at 1200 UTC over Lisbon, whereas Figure 3c shows the vertical wind speed profile simulated by Meso-NH at the fire's start point. In Figure 3b, it can be seen that air temperature exceeded 25.8 °C with a dew point temperature of around 16.8 °C near 100 m altitude. The figure also shows that the wind direction was from the north at lower levels and the southwest in the middle levels (wind barbs). Figure 3c shows two layers with more intense airflow; the first one was found lower than 1000 m altitude, and the second was between 4000 and 6000 m altitude. A wind speed of almost 9 m s^{-1} is simulated at 1500 UTC in the lower layer (≈600 m altitude) and 10 m s^{-1} at 1800 UTC (Figure 3c).

After that, there was a decrease in the wind magnitude, with values of 9 m s^{-1} at 2100 UTC, whereas at 0000 UTC, the wind speed decreased to 7.5 m s^{-1} at the same level. In the higher windy layer (4000–6000 m), the wind speed maximum was around 10 m s^{-1} during the entire period. This layer of maximum wind speed corresponds to the change in the wind direction shown in Figure 3b.

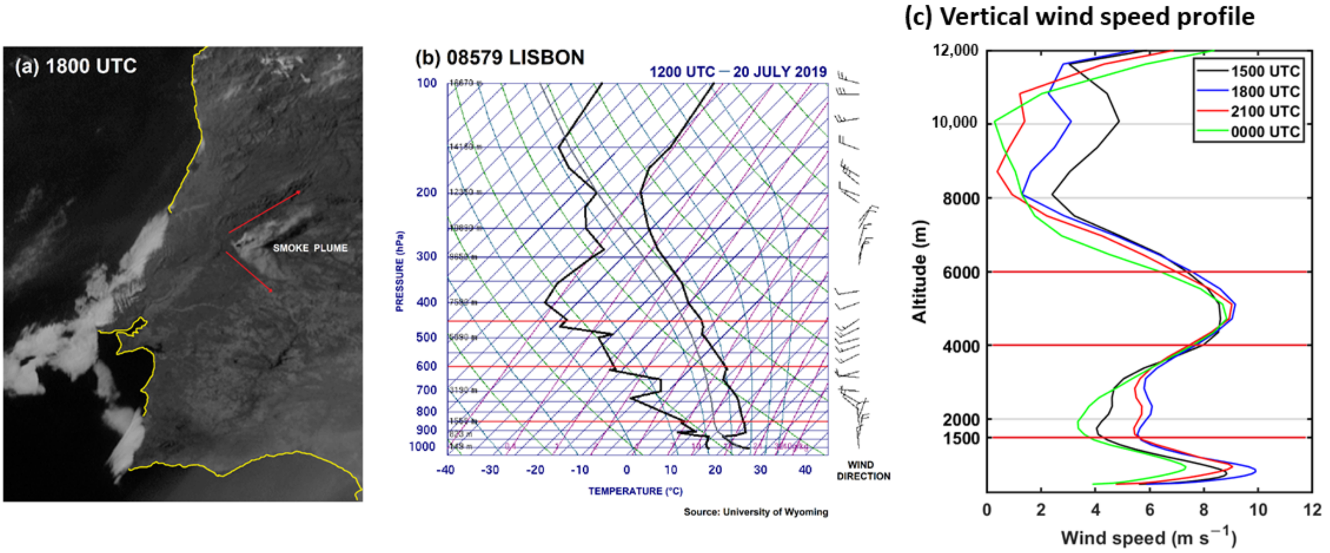

Figure 3. (**a**) Satellite images of the fire smoke plume over Vila de Rei's wildfire in the afternoon of 20 July 2019 at 1800 UTC; (**b**) Skew-T log-P diagram observation in Lisbon on 20 July 2019 at 1200 UTC; (**c**) Vertical wind speed profile at the fire's start point during 20 and 21 July 2019.

3.2. Model Verification

The model validation is made from a simple comparison between observed and simulated time series of the CTRL and EXP simulations. The meteorological variables at 2 m, namely the air temperature and relative humidity, as well as the wind gusts at 10 m, are considered in the validation (Figure 4). The comparison is made for the two closer meteorological stations during the period between 20 and 21 July 2019. The orange box represents the period simulated with the inner domain and the red box the more significant fire period.

The air temperature observed is higher than simulated in the afternoon of 20 July 2019 and in the morning of 21 July, with a maximum of 36 °C at 1400 UTC in Alvega (Figure 4a). At the same time, the maximum air temperature is 32.1 °C in Tomar (not shown). Considering the Tomar meteorological station, Figure 4b shows that the model well simulates values of relative humidity for the domain with 2500 m resolution. In Alvega, the minimum relative humidity observed is 27.2% (not shown) and 41.2% in Tomar (Figure 4b) at 1400 UTC on 20 July 2019. Therefore, the comparison of the observations shows that the air temperature and relative humidity simulated are close to the observations. Despite some overestimation of the wind speed at the Alvega station (not shown), the wind simulated in the inner domain of the EXP experiment is closer to the observations most of the time at the Tomar station. In Tomar (Figure 4c), the wind speed observed is 7.8 m s^{-1} at 1700 UTC on 20 July, which is underestimated by the model. However, in Alvega, the wind speed observed is 6.3 m s^{-1} at 1400 UTC (not shown). The comparison allows the use of higher resolution simulations to analyse the evolution of the airflow during the period.

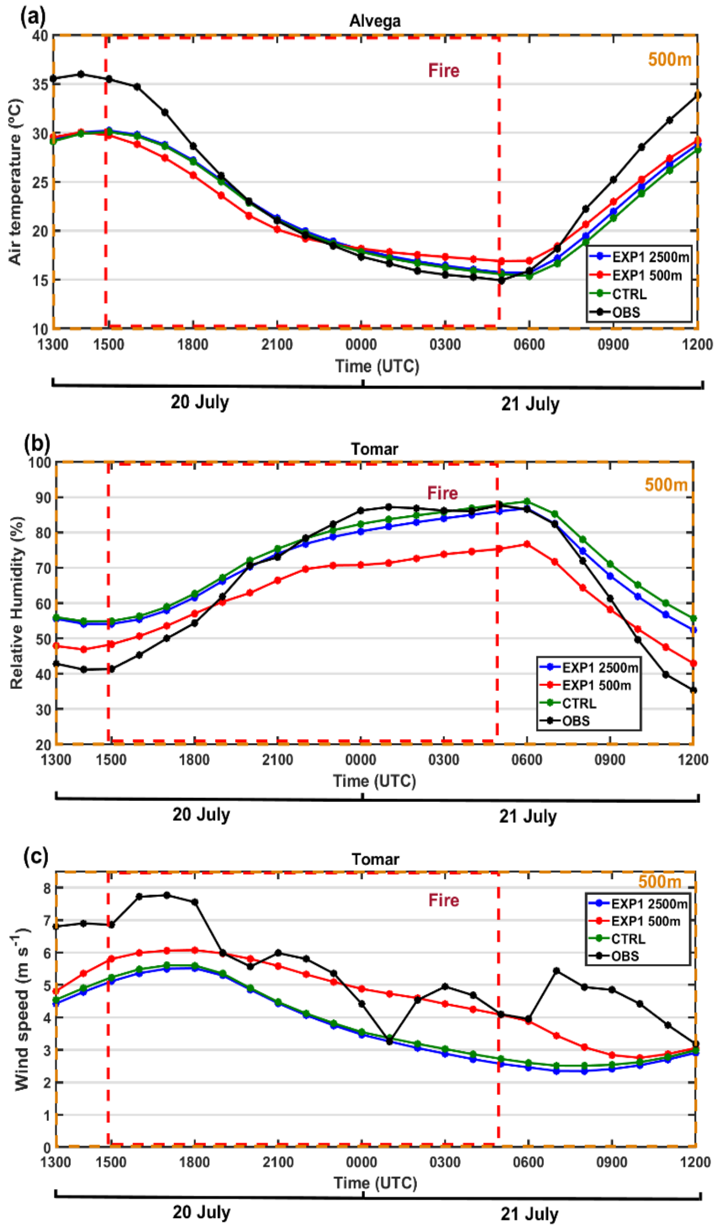

Figure 4. Comparison of the meteorological variables between the CTRL and EXP simulations with observations from the weather automatic stations during the inner domain period (orange box) and wildfire period (red box): (**a**) air temperature (°C) at 2 m in Alvega; (**b**) relative humidity (%) at 2 m in Tomar, and (**c**) wind speed (m s^{-1}) at 10 m in Tomar.

3.3. Synoptic Environment

Figure 5a shows the synoptic condition during the fire event in Vila de Rei. According to the mean sea level (MSL) pressure and wind speed at the surface on 20 July 2019 at 1800 UTC, the Azores anticyclone is centred south-eastward of the Azores archipelago (35° N, 25° W) with pressure values on the coastline of Portugal between 1015 and 1020 hPa. The winds are stronger near the coastline, coherent with the wind barbs shown in Figure 3c and observed over Lisbon. Moreover, the wind strength showed a maximum above 10 m s^{-1} and less than 4 m s^{-1} over the Iberian Peninsula. Figure 5a also shows a depression centred over eastern Iberia with pressure values lower than 1008 hPa. In order to better understand and characterise the Iberian depression, the mean sea level pressure simulated by the Meso-NH in the CTRL simulation is analysed (Figure 5b). It is possible to see the strong west–east pressure gradient between the coastline of Portugal, with 1018 hPa, and a low-pressure region over the Iberian Peninsula, which presents values lower than 1008 hPa. The MSL pressure pattern is similar to that reported in other studies on the summer circulation over the peninsula [18]. The vertical structure of air temperature, potential temperature, and the wind over the Iberian Peninsula are shown along the W–E cross-section marked as A-A′ in Figure 5b–f. Figure 5c shows high near-surface temperatures above 35 °C in the centre of the peninsula. The plot of potential temperature shows the existence of a well-mixed and deep boundary layer up to an altitude of more than 3000 m in central Iberia (Figure 5d). The strong boundary layer west–east potential temperature gradient over coastal land regions and the increase in the boundary layer height through the centre of the peninsula is very noticeable. Therefore, the atmospheric thermal structure clearly indicates the thermal origin of the depression, i.e., of the Iberian thermal low. In response to strong temperature and pressure gradients, stronger wind speeds occur along the coast during the afternoon of 20 July (Figure 5e,f), where the values reach more than 14 m s^{-1} at 1800 UTC (Figure 5f). In the peninsula's inner region, characterised by a very deep mixing layer and low horizontal pressure gradient, near the thermal low centre, the wind is weak, under 2 m s^{-1}.

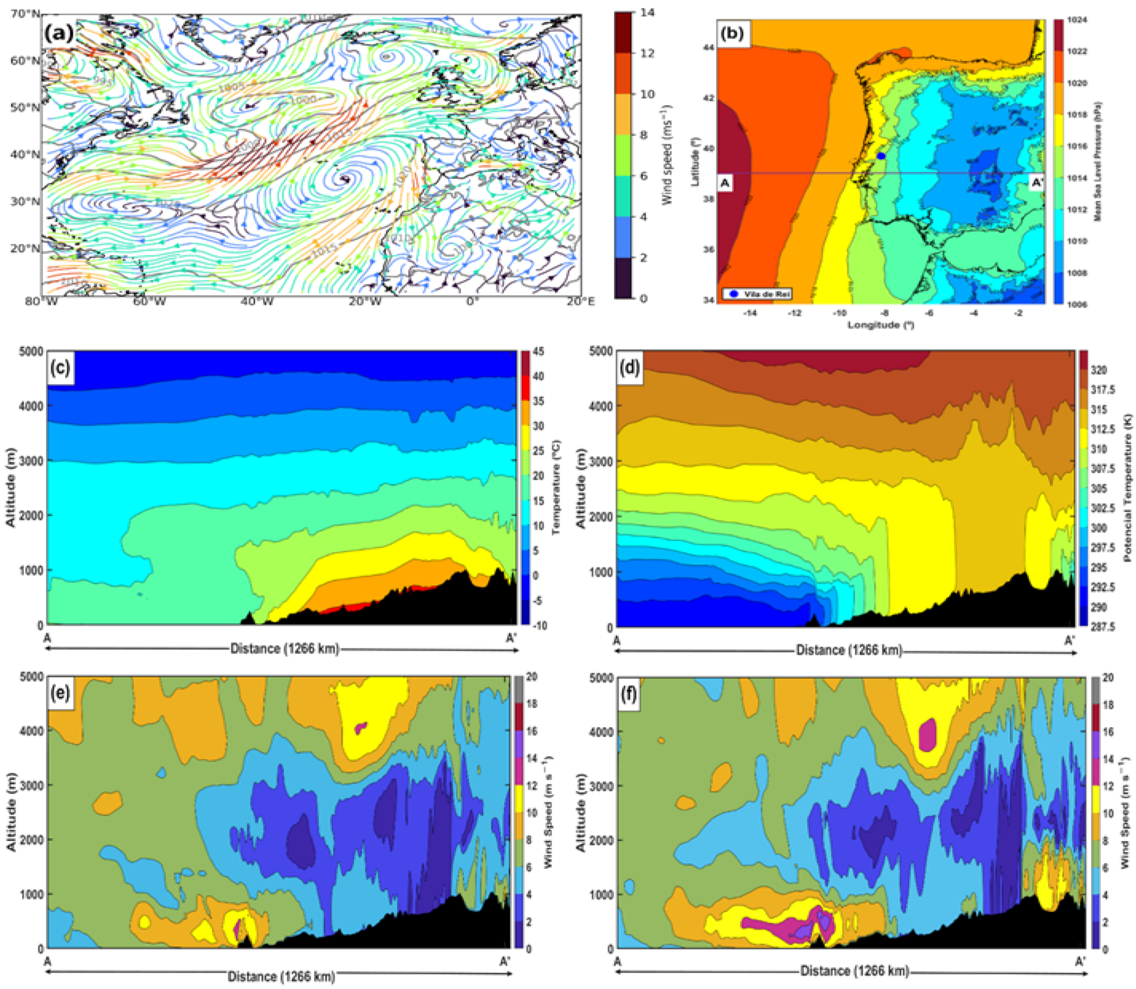

Figure 5. (**a**) Mean sea level pressure and surface wind speed at 1800 UTC on 20 July 2019, according to the ECMWF re-analyses; (**b**) Mean sea level pressure over the Iberian Peninsula from the Meso-NH simulation on 20 July 2019 at 1800 UTC; (**c**) Temperature at 1800 UTC; (**d**) Potential Temperature at 1800 UTC; and wind speed (**e**) at 1500 UTC and (**f**) at 1800 UTC.

3.4. Mesoscale Environment and Fire Weather Conditions

In order to identify the mesoscale conditions that influenced the fire behaviour, this section concentrates on the analysis of the fire weather variables at simulation with 2500 m resolution, followed by analysing the evolution of the high-resolution wind field (results from the 500 m resolution).

The fire started under high temperature and low relative humidity conditions that are relatively common during the summer period. Although temperatures around 40 °C were simulated and observed, in the south and central inner regions of the Iberian Peninsula, the air temperature near Vila de Rei was about 30 °C in the middle of the afternoon (1500 UTC, not shown) when the fire started. The air temperature decreased in the late afternoon, with values of 25 °C at 1800 UTC (Figure 6a) and a minimum of 20 °C at 0400 UTC (not shown). This evolution indicates that, during the period of fire spread, the meteorology did not favour higher temperatures throughout the night, as is sometimes observed during large fires in regions of complex terrain [19,20].

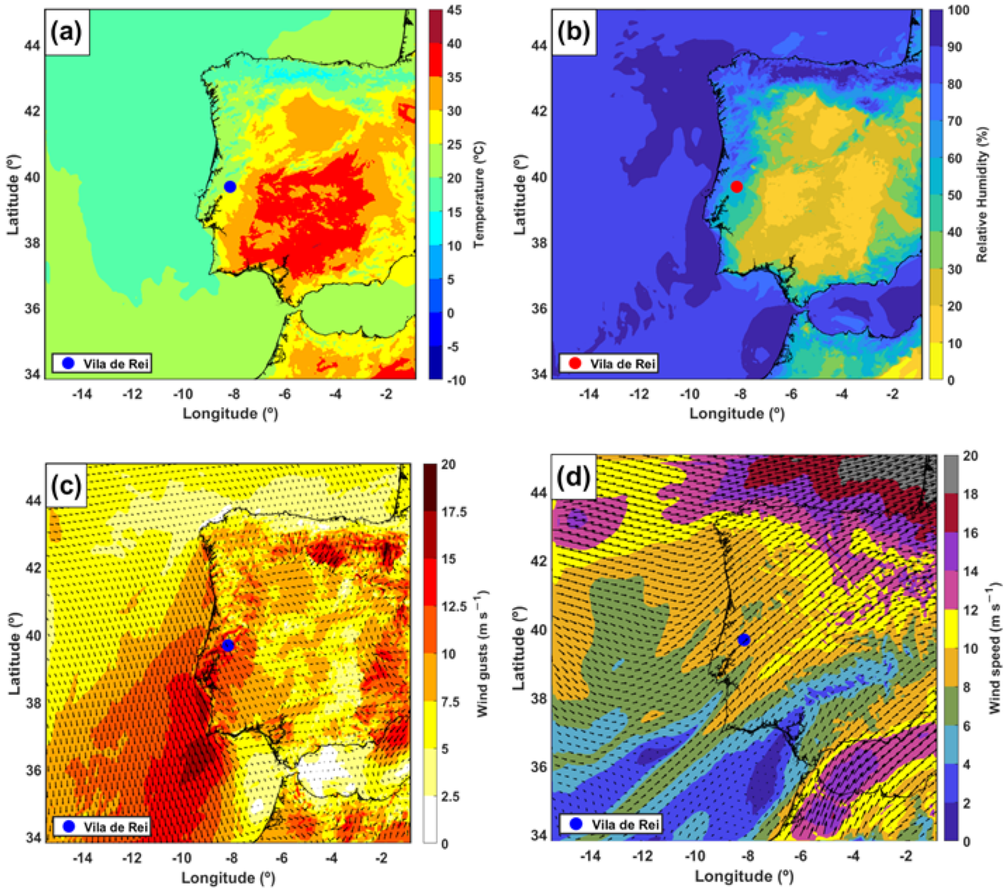

Figure 6. Fire weather conditions in the Iberian Peninsula at 1800 UTC on 20 July 2019 obtained from EXP results: (**a**) Air temperature at 2 m (°C); (**b**) relative humidity at 2 m; (**c**) wind gusts and wind direction (arrows) at 10 m; and (**d**) wind speed and direction (arrows) at 5000 m altitude.

The relative humidity field also followed a common evolution throughout the fire period. The model simulates an increase in the relative humidity in the afternoon, with values higher than 60% in northern Spain, and almost all Portuguese territory, whereas in southern Portugal and central and southern Spain, the values remain below 30% (Figure 6b). Furthermore, the relative humidity is higher on the western coast during the night and early morning (not shown).

The evolution of the wind field is analysed, taking into account the wind gust and the wind direction at 10 m over the Iberian Peninsula. The simulation shows that the northwest wind prevails over all of Portugal, with increasing intensity from the middle afternoon, namely in the southern region. Wind gusts from 5 m s^{-1} over the central Iberian Peninsula until 15 m s^{-1} in central and southwest coastal Portugal were simulated (not shown). At the end of the afternoon (1800 UTC), there is a generalised reduction of wind speed over the peninsula, except over some regions, in particular in the region of the Tagus valley south of Vila de Rei, where maximum wind gusts between 13 and 17 m s^{-1} are found (Figure 6c). The wind speed and direction at 5000 m altitude at 1800 UTC over the Iberian Peninsula are shown in Figure 6d. The figure shows the wind direction is predominantly from the southwest over the region of Vila de Rei, with wind speeds between 8 and 10 m s^{-1}.

Figure 7a shows the orography of the finer domain at 500 m resolution and the intersection of two vertical cross-sections with the surface. The EXP simulation wind speed is plotted (Figure 7b,c) on these two cross-sections so that the burned area is aligned with the two directions of the smoke plume (remember Figure 3a,b). At 2200 UTC, the wind field in the vertical section B–B′ (Figure 7b) shows a layer at around 500 m altitude, with a wind speed higher than 10 m s^{-1}. As seen, the surface of this vertical plane is middling flat and, in addition, the cross-section is aligned with the dominant lower tropospheric (wind direction, the wind speed profile is horizontally quite homogeneous).

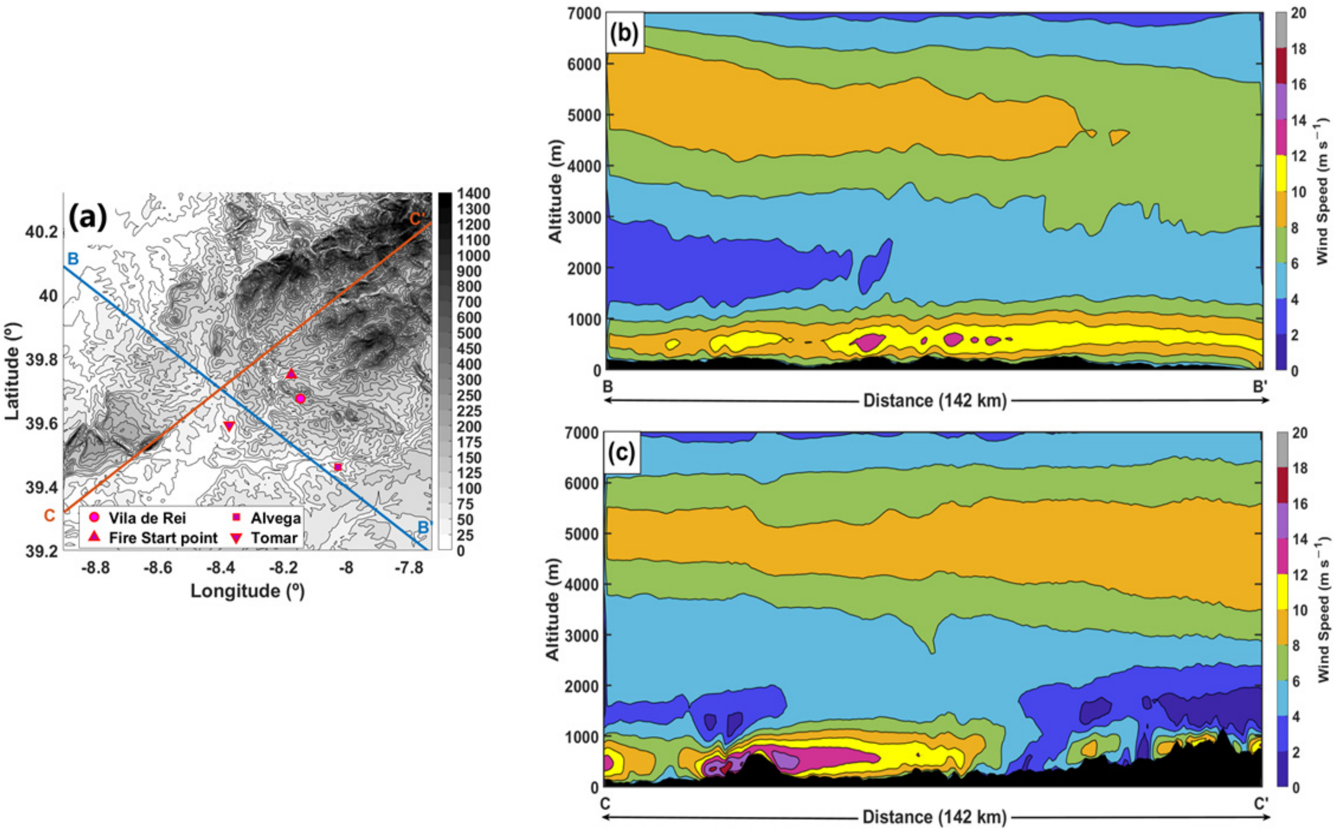

Figure 7. (**a**) Orography of the regional area; (**b**) Vertical cross-sections of the wind speed (m s^{-1}) by EXP simulation on 20 July 2019 at 2200 UTC along B–B′; (**c**) and C–C′.

The near-surface wind gusts and direction at the local burned area on 20 July 2019 are shown in Figure 8. The wind direction at 10 m is predominantly from the northwest during the entire period. It is noteworthy that the near-surface wind gusts in Vila de Rei's wildfire vary from 10 m s^{-1} up to 12.5 m s^{-1} at 1500 UTC, with the maximum up to 15 m s^{-1} (Figure 8a). The maximum wind speed of 15 m s^{-1} is found at 1800 UTC in the southeast of Vila de Rei (Figure 8b). Figure 8c, corresponding to 2100 UTC, indicates some locales southeast of Vila de Rei with the maximum wind values corresponding to the zone where the wildfire was active. The same figure shows the wind gusts (<7.5 ms^{-1}) in the northeast of the burned area. During the night, the wind weakens, with gusts below 10 m s^{-1} in most of the burned area at 0000 UTC on 21 July, except in some regions with a maximum of 12.5 m s^{-1} (Figure 8d).

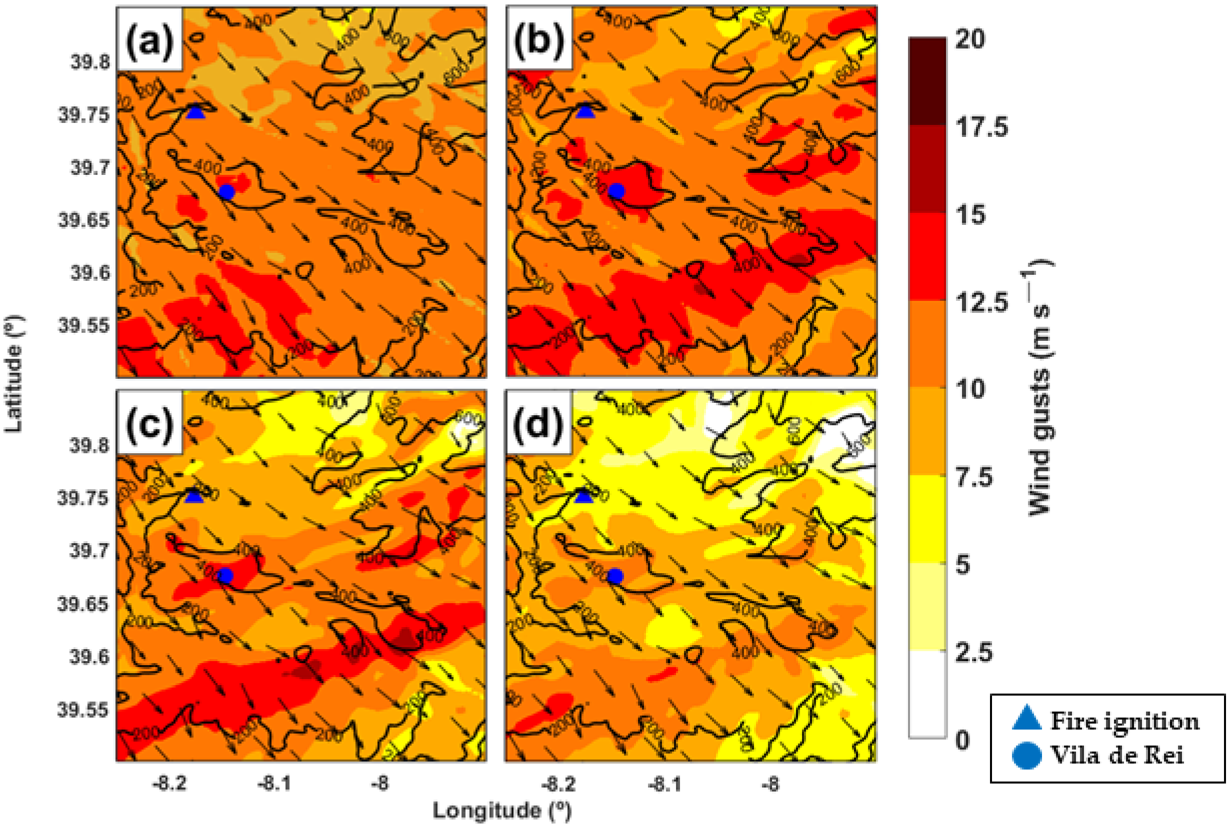

Figure 8. Wind gusts (coloured), wind direction (arrows), and orography (contour) of the local burned area by 500 m resolution on 20 July 2019 (**a**) at 1500 UTC, (**b**) 1800 UTC, (**c**) 2100 UTC, and (**d**) 0000 UTC on 21 July 2019.

The intersection of four vertical cross-sections of the wind speed field intersecting the burned area is shown in Figure 9 along SW–NE cross-sections during the time evolution of the fire. The wind speed reached between 8 and 10 m s^{-1} at 1500 UTC in the D–D′ section when the fire started (Figure 9a). In both the E–E′ and F–F′ sections, the wind speed reached 10 m s^{-1} near the surface at 1800 UTC and 2100 UTC, as shown in Figure 9b and Figure 9c, respectively. From Figure 9b, a maximum wind speed around 500 m altitude is simulated, with values less than 12 m s^{-1} at 1800 UTC. After that, the wind speed maximums are found inside some regions of values still higher than 12 m s^{-1} in the burned area of the F-F′ vertical cross-section at 2100 UTC (Figure 9c). Figure 9d shows that the wind speed is lower near the surface over the burned area in the G–G′ vertical cross-section, with values between 6 and 10 m s^{-1} at 0000 UTC on 21 July. Also, this figure indicates a decrease in the wind speed magnitude during the night. From this moment, the wind speed continues to decrease in magnitude for the next hours (not shown).

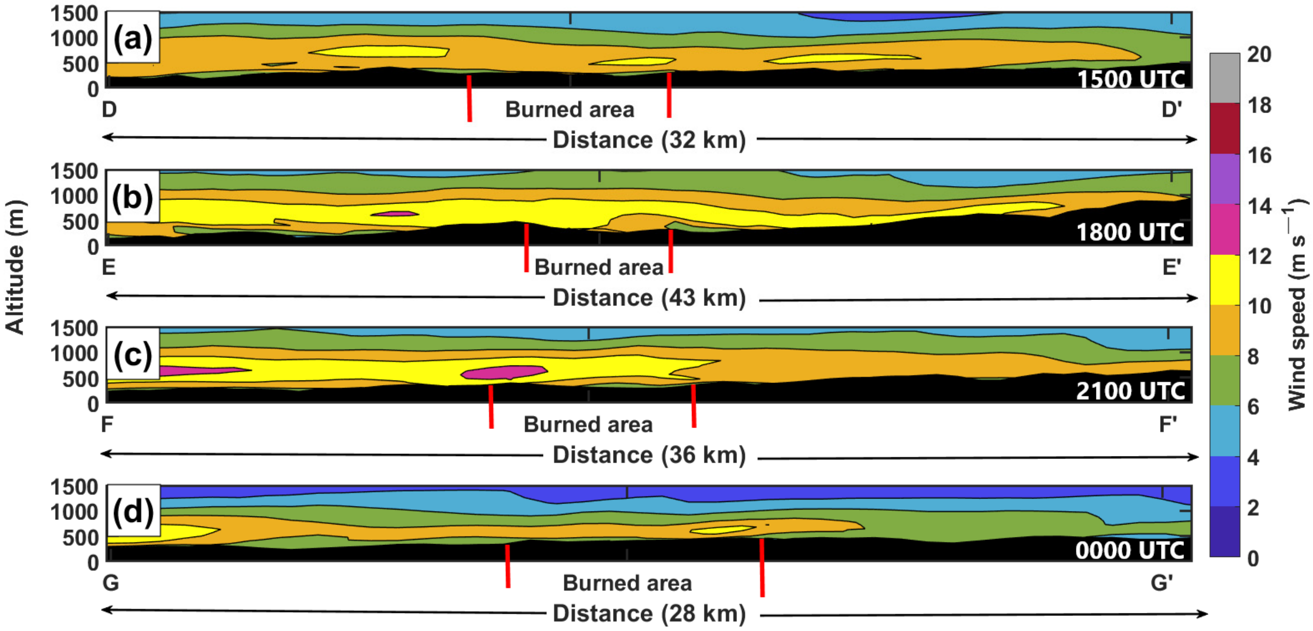

Figure 9. Wind Speed (contours) along the vertical cross sections by EXP simulation on 20 July 2019 (**a**) at 1500 UTC, (**b**) at 1800 UTC, (**c**) at 2100 UTC (**d**), and at 0000 UTC, with the burned area (red markers). The vertical cross-sections D–D′, E–E′, F–F′ and G–G′ show the wind speed vertical cross-sections (see Figure 2a for locations).

4. Discussion

The atmospheric conditions associated with the largest forest fire that occurred in Portugal in 2019 have been presented based on a set of numerical simulations with convection explicitly resolved and observational data.

In a synoptic-scale context, some weather patterns may be verified over the Iberian Peninsula in the summer season. The lower temperatures and higher relative humidity over the northern and western Iberian Peninsula are due to northwest dominant flow, which is a consequence of the interactions between the large-scale west mid-latitude circulation, the Azores anticyclone centred in the North Atlantic Ocean, and the breeze system organised at a peninsular scale. Over the southern and eastern Iberian Peninsula, dry air and higher temperatures during the afternoon force a thermal low system, which is also called the Iberian thermal low. The position of these two systems creates a strong seasonal northwest wind over Portugal, locally known as "Nortada", and a coastal low-level jet [50,51]. This phenomenon, which is more frequent in summer, is induced by the contrast between the daytime heating of the sea and land in the early afternoon, which leads to an increase in wind intensity on the west coast of Portugal. Vila de Rei county is found in a region where the occurrence of large fires is favoured, also characterised as the southwest cluster (SW_CLU) [52], and presents the same atmospheric circulation identified in this study. Here, the wind gusts are simulated near the surface, with values between 15 and 17.5 m s^{-1}, and the mean wind speed reached 10 m s^{-1} near 600 m altitudes. In relation to the coastal low-level jet, the results presented are coherent with other studies for wind speed field at the surface [50] and the altitudes of the maximum wind speed [51].

A layer with strong northwest winds was reproduced below 1 km altitude. This layer favoured the transport of the smoke plume to southern Portugal, previously identified by [34], as seen in Figure 3. In addition, a strong southwest wind at higher altitudes is responsible for the second smoke plume north-eastward of Vila de Rei, as observed in the satellite images (Figure 3).

The meteorological observations showed a maximum air temperature above 36 °C, a minimum relative humidity around 40%, and a wind speed below 7 m s^{-1}, values that were well reproduced by the numerical simulations. According to the simulations, the wind gusts in wildfire areas varied between 10 and 15 m s^{-1}, with maximum values during the afternoon. The strong northwest wind was the main factor inducing the high spread rate of the fire front and increased the burned area in a short time. The fire propagation was clearly driven by the wind field, well-marked by the intensification of the airflow on the burning slope. The burned area in Vila de Rei demonstrates a shape similar to many wind-driven fires, with the fire's centre spreading faster than the flanks, which propagated in the direction of the prevailing wind.

Although the fire weather conditions over the Vila de Rei region and the wind gusts did not reach values more extreme than those reported during other forest-fire events, for example, in central Greece [16] or on Madeira island [20], the wildfire propagated faster than in those events. In the case of central Greece, for example, the maximum air temperature was 39 °C, the minimum relative humidity was 21%, and the maximum wind gusts were 25.2 m s^{-1}. On Madeira Island, the air temperature was above 35 °C, the relative humidity values were around 15%, and the wind gust maximum reached 30 m s^{-1}.

The study confirms that the connection between large scale environment, mesoscale circulation, and complex terrain can create a variety of significant effects on fire, including the intensification of airflow near the surface, which can produce the development of large fires in a short time, mainly when the topography is aligned with the synoptic flow.

5. Conclusions

This study aimed to identify the atmospheric conditions associated with the largest forest fire in Portugal in 2019 using simulations with convection explicitly resolved. The fire mainly spread along a valley and propagated onto the surrounding hills, a region characterised by the presence of pine trees and eucalyptus.

In the synoptic conditions, the interaction between the atmospheric circulation system, namely the Azores anticyclone centred near the Azores archipelago and the Iberian thermal low produces an effect in wind intensity on the west coast of Portugal known as the coastal low-level jet. This phenomenon is observed in the lowest troposphere, with a maximum wind speed situated at 600 m altitude. A change in surface wind direction was observed, prevailing from the northwest at lower levels, which favoured the transport of the smoke plume to southern Portugal, while as height increased, it shifted the direction to the southwest, inducing the transport of the smoke plume to the northeast of Vila de Rei, as observed in the satellite images.

The evolution of the event was driven by a combination of factors that led to enhanced fire danger, namely the orographic aspects and airflow configuration. The burned area in Vila de Rei expanded due to the intensification of the airflow near the surface in the first hours and produced a wind-driven fire event characterised by the rapid spread of the fire front in a short time.

The Meso-NH model was able to represent the fire weather conditions. The increase in the resolution to 500 m enabled a better representation of the surface, as well as the interaction of atmospheric flow in the region with the surface and the wind behaviour to understand the evolution of the burned area over the period. The large domain covering the Iberian Peninsula allowed us to study the large mesoscale phenomena, namely the Iberian thermal low.

The case study contributes to improving the knowledge of large fire occurrences in Portugal, the European country most affected by forest fires. The numerical modelling helped to understand the dynamics behind the swift burning behaviour. Weather pattern recognition can facilitate the identification of favourable conditions for the development of large fires, which is important to prevent fires and improve firefighting.

The numerical coupling between a fire model and an atmospheric model allows a better understanding of the mechanisms driving the fire spread and may have consequences for the operational sector [35,53,54]. Thus, as further work, the authors suggest the use of coupled simulations for a better understanding of the interaction between the fire weather conditions and orographic effects influencing the fire propagation, which was not the objective of this study.

Author Contributions: Conceptualisation, C.P. and F.T.C.; methodology, C.P., N.A., M.P., V.S. and F.T.C.; software, C.P., N.A., M.P., V.S. and F.T.C.; formal analysis, C.P. and F.T.C.; investigation, C.P.; resources, F.T.C. and R.S.; data curation, C.P., N.A., M.P. and V.S.; writing—original draft preparation, C.P.; writing—review and editing, C.P., N.A., M.P., V.S., F.T.C. and R.S.; visualisation, C.P., N.A., M.P. and V.S.; supervision, F.T.C.; project administration, F.T.C. and R.S.; funding acquisition, F.T.C. and R.S. All authors have read and agreed to the published version of the manuscript.

Funding: This research was funded by the European Union through the European Regional Development Fund in the framework of the Interreg V A Spain—Portugal program (POCTEP) through the CILIFO project (Ref.: 0753-CILIFO-5-E), FIREPOCTEP project (0756-FIREPOCTEP-6-E), RH.VITA project (ALT20-05-3559-FSE-000074) and also by national funds through FCT—Foundation for Science and Technology, I.P. under the PyroC.pt project (Refs. PCIF/MPG/0175/2019), ICT project (Refs. UIDB/04683/2020 and UIDP/04683/2020).

Institutional Review Board Statement: Not applicable.

Informed Consent Statement: Not applicable.

Data Availability Statement: Not applicable.

Acknowledgments: We want to thank Filippe Santos (Universidade de Évora; Instituto de Ciências da Terra—ICT) for making the satellite images available. The authors are grateful to the Portuguese meteorological service (IPMA) for providing meteorological data and to the European Centre for Medium-Range Weather Forecasts (ECMWF) for the provided meteorological analysis.

Conflicts of Interest: The authors declare no conflict of interest.

References

1. Pereira, M.G.; Trigo, R.M.; da Camara, C.C.; Pereira, J.M.C.; Leite, S.M. Synoptic patterns associated with large summer forest fires in Portugal. *Agric. For. Meteorol.* **2006**, *129*, 11–25. [CrossRef]
2. Amraoui, M.; Pereira, M.G.; DaCamara, C.C.; Calado, T.J. Atmospheric conditions associated with extreme fire activity in the Western Mediterranean region. *Sci. Total Environ.* **2015**, *524–525*, 32–39. [CrossRef]
3. Werth, P.A. Critical Fire Weather Patterns. In *Synthesis of Knowledge of Extreme Fire Behavior: Volume I for Fire Managers*; United States Department of Agriculture Forest Service: Washington, DC, USA, 2011; pp. 25–48.
4. Keeley, J.E.; Syphard, A.D. Twenty-first century California, USA, wildfires: Fuel-dominated vs. wind-dominated fires. *Fire Ecol.* **2019**, *15*, 24. [CrossRef]
5. Whiteman, C.D. Fire Weather and Smoke Management. In *Mountain Meteorology: Fundamentals and Applications*, 21st ed.; Oxford University Press: New York, NY, USA, 2000; pp. 237–272.
6. Clements, C.B.; Seto, D. Observations of Fire–Atmosphere Interactions and Near-Surface Heat Transport on a Slope. *Bound.-Layer Meteorol.* **2015**, *154*, 409–426. [CrossRef]
7. Vanella, M.; McGrattan, K.; McDermott, R.; Forney, G.; Mell, W.; Gissi, E.; Fiorucci, P. A Multi-Fidelity Framework for wildland Fire Behavior Simulations over Complex Terrain. *Atmosphere* **2021**, *12*, 273. [CrossRef]
8. McCarthy, E.F. Forest fires and storm movement. *Mon. Weather Rev.* **1924**, *52*, 257–259. [CrossRef]
9. Byram, G.M. *Atmospheric Conditions Related to Blow-Up Fires*; Station Paper SE-SP-35; USDA-Forest Service, South-Eastern Forest Experiment Station: Asheville, NC, USA, 1954; 36p.
10. Sharples, J. Review of formal methodologies for wind-slope correction of wildfire rate of spread. *Int. J. Wildland Fire* **2008**, *17*, 179–193. [CrossRef]
11. Brewer, M.J.; Clements, C.B. The 2018 Camp Fire: Meteorological Analysis Using In Situ Observations and Numerical Simulations. *Atmosphere* **2020**, *11*, 47. [CrossRef]
12. Moritz, M.A.; Moody, T.J.; Krawchuk, M.A.; Hughes, M.; Hall, A. Spatial variation in extreme winds predicts large wildfire locations in chaparral ecosystems. *Geophys. Res. Lett.* **2010**, *37*, L04801. [CrossRef]
13. Jin, Y.; Randerson, J.T.; Capps, S.; Hall, A.; Faivre, N.; Goulden, M.L. Contrasting controls on wildland fires in Southern California during periods with and without Santa Ana events. *J. Geophys. Res. Biogeosci.* **2014**, *119*, 432–450. [CrossRef]
14. Ruffault, J.; Moron, V.; Trigo, R.M.; Curta, T. Daily synoptic conditions associated with large fire occurrence in Mediterranean France: Evidence for a wind-driven fire regime. *Int. J. Clim.* **2017**, *37*, 524–533. [CrossRef]
15. Lagouvardos, K.; Kotroni, V.; Giannaros, T.M.; Dafis, S. Meteorological Conditions Conducive to the Rapid Spread of the Deadly Wildfire in Eastern Attica, Greece. *Bull. Am. Meteorol. Soc.* **2019**, *100*, 2137–2145. [CrossRef]

16. Kartsios, S.; Karacostas, T.; Pytharoulis, I.; Dimitrakopoulos, A.P. Numerical investigation of atmosphere-fire interactions during high-impact wildland fire events in Greece. *Atmos. Res.* **2020**, *247*, 105253. [CrossRef]
17. Hoinka, K.P.; Gaertner, M.; Castro, M. Iberian thermal lows in a changed climate. *Q. J. R. Meteorol. Soc.* **2007**, *133*, 1113–1126. [CrossRef]
18. Salgado, R.; Miranda, P.M.A.; Lacarrère, P.; Noilhan, J. Boundary layer development and summer circulation in Southern Portugal. *Tethys* **2015**, *12*, 33–44. [CrossRef]
19. Nauslar, N.J.; Abatzoglou, J.T.; Marsh, P.T. The 2017 North Bay and Southern California Fires: A Case Study. *Fire* **2018**, *1*, 18. [CrossRef]
20. Couto, F.T.; Salgado, R.; Guiomar, N. Forest Fires in Madeira Island and the Fire Weather Created by Orographic Effects. *Atmosphere* **2021**, *12*, 827. [CrossRef]
21. Potter, B.E. Column/Plume Dynamics. In *Synthesis of Knowledge of Extreme Fire Behaviour: Vol I for Fire Managers*; U.S. Department of Agriculture, Forest Service, Pacific Northwest Research Station: Corvallis, OR, USA, 2011; pp. 73–80.
22. Kochanski, A.K.; Jenkins, M.A.; Mandel, J.; Beezley, J.D.; Krueger, S.K. Real time simulation of 2007 Santa Ana fires. *For. Ecol. Manag.* **2013**, *294*, 136–149. [CrossRef]
23. Bova, A.; Mell, W.; Hoffman, C. A comparison of level set and marker methods for the simulation of wildland fire front propagation. *Int. J. Wildland Fire* **2015**, *25*, 229–241. [CrossRef]
24. Bakhshaii, A.; Johnson, E. A review of a new generation of wildfire−atmosphere modeling. *Can. J. For. Res.* **2019**, *49*, 565–574. [CrossRef]
25. Parente, J.; Pereira, M.G.; Amraoui, M.; Tedim, F. Negligent and intentional fires in Portugal: Spatial distribution characterization. *Sci. Total Environ.* **2018**, *624*, 424–437. [CrossRef]
26. Trigo, R.; Pereira, J.; Pereira, M.; Mota, B.; Calado, T.; Camara, C.D.; Santo, F. Atmospheric conditions associated with the exceptional fire season of 2003 in Portugal. *Int. J. Clim.* **2006**, *26*, 1741–1758. [CrossRef]
27. Pereira, M.G.; Malamud, B.D.; Trigo, R.M.; Alves, P.I. The history and characteristics of the 1980–2005 Portuguese rural fire database. *Nat. Hazards Earth Syst. Sci.* **2011**, *11*, 3343–3358. [CrossRef]
28. Couto, F.T.; Iakunin, M.; Salgado, R.; Pinto, P.; Viegas, T.; Pinty, J.-P. Lightning modelling for the research of forest fire ignition in Portugal. *Atmos. Res.* **2020**, *242*, 104993. [CrossRef]
29. Carmo, M.; Ferreira, J.; Mendes, M.; Silva, Á.; Silva, P.; Alves, D.; Reis, L.; Novo, I.; Xavier Viegas, D. The climatology of extreme wildfires in Portugal, 1980–2018: Contributions to forecasting and preparedness. *Int. J. Clim.* **2021**, *42*, 3123–3146. [CrossRef]
30. Turco, M.; Jerez, S.; Augusto, S.; Tarín-Carrasco, P.; Ratola, N.; Jiménez-Guerrero, P.; Trigo, R.M. Climate drivers of the 2017 devastating fires in Portugal. *Sci. Rep.* **2019**, *9*, 13886. [CrossRef]
31. Pinto, P.; Silva, Á.P.; Viegas, D.X.; Almeida, M.; Raposo, J.; Ribeiro, L.M. Influence of Convectively Driven Flows in the Course of a Large Fire in Portugal: The Case of Pedrógão Grande. *Atmosphere* **2022**, *13*, 414. [CrossRef]
32. Trigo, R.M.; García-Herrera, R.; Díaz, J.; Trigo, I.F.; Valente, M.A. How exceptional was the early August 2003 heatwave in France? *Geophys. Res. Lett.* **2005**, *32*, L10701. [CrossRef]
33. Rego, F.; Fernandes, P.; Silva, J.S.; Azevedo, J.C.; Moura, J.M.; Oliveira, E.; Cortes, R.; Viegas, D.X.; Caldeira, D.; Duarte Santos, F. Relatório de Avaliação do Incêndio de Fundada (Vila de Rei—Mação); Observatório Técnico Independente, Assembleia da República, Lisboa. 2020. Available online: https://www.parlamento.pt/Documents/2020/fevereiro/FINAL-Relatorio-de-Vila-de-Rei.pdf (accessed on 6 September 2021).
34. Salgueiro, V.; Costa, M.J.; Guerrero-Rascado, J.I.; Couto, F.T.; Bortoli, D. Characterization of forest fire and Saharan desert dust aerosols over south-western Europe using a multi-wavelength Raman LIDAR and Sun-photometer. *Atmos. Environ.* **2021**, *252*, 118346. [CrossRef]
35. Filippi, J.-B.; Bosseur, F.; Mari, C.; Lac, C. Simulation of a Large Wildfire in a Coupled Fire-Atmosphere Model. *Atmosphere* **2018**, *9*, 218. [CrossRef]
36. Weather Spark—Condições Meteorológicas no Verão em Vila de Rei. Available online: https://pt.weatherspark.com/s/32215/1/Condi%C3%A7%C3%B5es-meteorol%C3%B3gicas-m%C3%A9dias-no-ver%C3%A3o-em-Vila-de-Rei-Portugal#Figures-WindDirection (accessed on 6 December 2021).
37. Lourenço, L. Tipos de tempo correspondentes aos grandes incêndios florestais ocorridos em 1986 no centro de Portugal. *Finisterra* **1988**, *46*, 251–270. [CrossRef]
38. Ferreira-Leite, F.; Bento-Gonçalves, A.; Lourenço, L. Grandes incêndios florestais em Portugal Continental. Da história recente à atualidade. *Cadernos de Geografia* **2012**, *30–31*, 81–86. [CrossRef]
39. Ferreira-Leite, F.; Lourenço, L.; Bento-Gonçalves, A. Large forest fires in mainland Portugal, brief characterization. *Mediterranee* **2013**, *121*, 53. [CrossRef]
40. Alexander, M.E.; Thorburn, W.R. Chapter 4—LACES: Adding an "A" for Anchor point(s) to the LCES wildland firefighter safety system. In *Current International Perspectives on Wildland Fires, Mankind and the Environment*, 1st ed.; Leblon, B., Alexander, M.E., Eds.; Nova Science Publishers: Hauppauge, NY, USA, 2015; pp. 121–144.
41. Fernandes, A. Diretiva Operacional Nacional No. 2—DECIR: Dispositivo Especial de Combate a Incêndios Rurais 2021. Autoridade Nacional da Emergência e Proteção Civil. 2021. Available online: http://www.prociv.pt/bk/PROTECAOCIVIL/LEGISLACAONORMATIVOS/OUTROSNORMATIVOSDIRETIVAS/Documents/DON_2_DECIR_2021.pdf (accessed on 11 May 2022).

42. Lac, C.; Chaboureau, J.-P.; Masson, V.; Pinty, J.-P.; Tulet, P.; Escobar, J.; Leriche, M.; Barthe, C.; Aouizerats, B.; Augros, C.; et al. Overview of the Meso-NH model version 5.4 and its applications. *Geosci. Model Dev.* **2018**, *11*, 1929–1969. [CrossRef]
43. Champeaux, J.L.; Masson, V.; Chauvin, F. ECOCLIMAP: A global database of land surface parameters at 1 km resolution. *Meteorol. Appl.* **2005**, *12*, 29–32. [CrossRef]
44. Cuxart, J.; Bougeault, P.; Redelsperger, J.L. A turbulence scheme allowing for mesoscale and large-eddy simulations. *Q. J. R. Meteorol. Soc.* **2000**, *126*, 1–30. [CrossRef]
45. Verrelle, A.; Ricard, D.; Lac, C. Sensitivity of high-resolution idealized simulations of thunderstorms to horizontal resolution and turbulence parametrization. *Q. J. R. Meteorol. Soc.* **2015**, *141*, 433–448. [CrossRef]
46. Pergaud, J.; Masson, V.; Malardel, S.; Couvreux, F. A parameterization of dry thermals and shallow cumuli for mesoscale numerical weather prediction. *Bound.-Layer Meteorol.* **2009**, *132*, 83–106. [CrossRef]
47. Pinty, J.-P.; Jabouille, P. A mixed-phase cloud parameterization for use in mesoscale non-hydrostatic model: Simulations of a squall line and of orographic precipitations. In Proceedings of the Conference on Cloud Physics, Everett, WA, USA, 17–21 August 1998; American Meteorological Society: Boston, MA, USA, 1999; pp. 217–220.
48. Masson, V.; Le Moigne, P.; Martin, E.; Faroux, S.; Alias, A.; Alkama, R.; Belamari, S.; Barbu, A.; Boone, A.; Bouyssel, F.; et al. The SURFEXv7.2 land and ocean surface platform for coupled or offline simulation of earth surface variables and fluxes. *Geosci. Model Dev.* **2013**, *6*, 929–960. [CrossRef]
49. Anderson, H.E. *Aids to Determining Fuel Models for Estimating fire Behaviour*; Gen. Tech. Rep. INT-122; U.S. Department of Agriculture, Forest Service, Intermountain Forest and Range Experiment Station: Ogden, UT, USA, 1982.
50. Soares, P.M.M.; Cardoso, R.M.; Semedo, Á.; Chinita, M.J.; Ranjha, R. Climatology of the Iberia coastal low-level wind jet: Weather research forecasting model high-resolution results. *Tellus A* **2014**, *66*, 22377. [CrossRef]
51. Lima, D.C.A.; Soares, P.M.M.; Nogueira, M.; Semedo, A. Global coastal low-level wind jets revisited through the new ERA5 re-analysis. *Int. J. Clim.* **2021**, *42*, 4491–4507. [CrossRef]
52. Trigo, R.M.; Sousa, P.M.; Pereira, M.G.; Rasilla, D.; Gouveia, C.M. Modelling wildfire activity in Iberia with different atmospheric circulation weather types. *Int. J. Clim.* **2016**, *36*, 2761–2778. [CrossRef]
53. Peace, M.; Mattner, T.; Mills, G.; Kepert, J.; McCaw, L. Coupled Fire–Atmosphere Simulations of the Rocky River Fire Using WRF-SFIRE. *J. Appl. Meteorol. Clim.* **2016**, *55*, 1151–1168. [CrossRef]
54. Ghaderi, M.; Ghodrat, M.; Sharples, J.J. LES Simulation of Wind-Driven Wildfire Interaction with Idealized Structures in the Wildland-Urban Interface. *Atmosphere* **2021**, *12*, 21. [CrossRef]